Applied Catalysis B: Environmental 196 (2016) 41–49

Contents lists available at ScienceDirect

Applied Catalysis B: Environmental

journal homepage: www.elsevier.com/locate/apcatb

Hydroprocessing of carinata oil for hydrocarbon biofuel over Mo-Zn/Al_2O_3

Xianhui Zhao[a], Lin Wei[a,*], Shouyun Cheng[a], Ethan Kadis[b], Yuhe Cao[a], Eric Boakye[c], Zhengrong Gu[a], James Julson[a]

[a] Department of Agricultural and Biosystems Engineering, South Dakota State University, Brookings, SD 57007, USA
[b] Department of Chemical Engineering, University of Massachusetts: Amherst, Amherst, MA 01003, USA
[c] Department of Chemistry and Biochemistry, South Dakota State University, Brookings, SD 57007, USA

ARTICLE INFO

Article history:
Received 9 January 2016
Received in revised form 10 May 2016
Accepted 10 May 2016
Available online 11 May 2016

Keywords:
Hydroprocessing
Carinata oil
Hydrocarbon biofuel
Mo-Zn/Al_2O_3
Batch reactor

ABSTRACT

Hydroprocessing of carinata oil over an Al_2O_3 supported Mo-Zn catalyst in a batch reactor at 350 °C with an initial H_2 pressure of 300 psi was carried out to produce hydrocarbon biofuel. A series of Mo-Zn/Al_2O_3 catalysts with different Zn/Mo molar ratios (0, 1, 2, 3, ∞) were prepared and characterized using XRD, FT-IR, BET and TEM. The effects on the physicochemical properties and yield of products from using no catalyst and Al_2O_3 based catalysts were discussed. The introduction of Mo and/or Zn did not change the crystalline structure of Al_2O_3. The combining of Mo and Zn on Al_2O_3 improved catalytic performance and was helpful to improve some of the physicochemical properties of hydrocarbon biofuel including hydrocarbon content, moisture content, density, total acid number and higher heating value (HHV). The catalyst which exhibited the best catalytic performance had a Zn/Mo molar ratio of 2:1. At the 2:1 ratio of Zn/Mo, the hydrocarbon biofuel produced displayed the highest hydrocarbon content (81.05%) and the lowest moisture content, and the highest sum content of CO and CO_2 in the gas produced. The introduction of Mo and Zn on Al_2O_3 was helpful for the hydroprocessing of carinata oil for hydrocarbon biofuel production.

1. Introduction

More than 80% of all petroleum extracted from the earth is processed as fuels including jet fuel, gasoline, diesel and other fuel oils. The depletion of finite oil reserves and increase in the greenhouse gas emissions is contributed to the excessive use of petroleum. Due to concerns of sustainability, environmental impact, increased global population and geopolitical stability, there is a growing political, social and economic interest for the development of alternative fuel sources. Biomass such as vegetable oilseed is usually used to produce carbon-neutral biofuel. Burning biofuel does not increase the CO_2 concentration in the atmosphere [1–4]. In recent years, concerns of resource competition between food and energy crops have been growing, which lead to a major interest in the development of biofuel production from a variety of non-food crops [5,6]. Brassica carinata is non-food crop which is an arid-resistant species [1]. It is commonly referred to as Ethiopian mustard or Abyssinian. Brassica carinata is highly drought and heat tolerant, and resistant to aphids, flea beetles and blackleg disease [7]. The positive agronomic attributes of the carinata oilseed make it compatible with fallow cropping and off-season cropping. The U.S. military has shown an interest in the carinata oilseed feedstocks and begun flight trials with carinata based jet fuel in 2012 [8]. Field tests of Brassica carinata commercial varieties have been successful across North Dakota, Montana, Mississippi and Florida in the United States [9].

There are several common methods to convert biomass to biofuel, such as fermentation, pyrolysis and upgrading, gasification, transesterification, catalytic cracking, and hydroprocessing [10]. Among these above methods, the thermochemical techniques used for vegetable oil conversion to biofuel include transesterification, catalytic cracking, and hydroprocessing. Due to the undesirable properties produced via transesterification such as low oxidative stability of biodiesel, and the low biofuel yield obtained from catalytic cracking of vegetable oil, hydroprocessing is an effective method to convert vegetable oil to biofuel even though the introduction of hydrogen contributes a portion of the processing cost [11]. Hydroprocessing is a widely used technology applied in petroleum refineries, whereas oxygen can be removed through three pathways. The first pathway, hydro-decarbonylation pro-

* Corresponding author.
E-mail address: lin.wei@sdstate.edu (L. Wei).

http://dx.doi.org/10.1016/j.apcatb.2016.05.020
0926-3373/

duces CO and H_2O. The second pathway, hydro-decarboxylation produces CO_2; and the last pathway, hydro-dewatering produces H_2O [12,13]. Zarchin et al. [12] studied the hydroprocessing of soybean oil over nickel-phosphide supported catalyst and 47% of oxygen was removed as CO and CO_2 from triglycerides.

Catalyst plays a significant role in the hydroprocessing of vegetable oil and commercial hydrotreatment catalysts such as Co-Mo/Al_2O_3 have been studied to investigate the hydrodeoxygenation of oxygen containing compounds [13]. The catalysts of CoMo and NiMo supported on Al_2O_3 had a high surface area, stable chemical properties and good mechanical properties. The loading of an acidic oxide MoO_3 to the Al_2O_3 support could increase the acidity due to the molybdate anions preferentially reacting with the basic hydroxyl groups on the Al_2O_3 support [14]. MoO_x, an oxide form of a transition metal, exhibited variable valence and might possess the ability for the activation of oxy-groups in oxygenates [15]. Srifa et al. [16] studied the hydrodeoxygenation of palm oil over the Al_2O_3 supported monometallic catalysts (Ni, Co, Pt and Pd) in a trickle-bed reactor at 330 °C and H_2 pressure of 5 MPa to produce green diesel. The deoxygenation of palm oil was proposed by the initial hydrogenation of unsaturated triglycerides to saturated triglycerides. Then, fatty acids and propane were formed through the hydrogenolysis of saturated triglycerides. Finally, green diesel was obtained through the deoxygenation of free fatty acids on the metallic sites of the catalysts. Krar et al. [17] studied the hydrotreating of sunflower oil over Co-Mo/Al_2O_3 catalyst to produce biofuel. The hydroprocessing parameters were: temperature (300–380 °C) and total pressure (20–80 bar). It was demonstrated that the Co-Mo/Al_2O_3 catalyst was suitable for the conversion of sunflower oil to new generation biofuel. The yield of the high paraffin containing (> 99%) gas oil boiling range product was between 73.7% and 73.9%. $ZnCl_2$ is a moderate strength Lewis acid with an effective cost and is proved to modify the zeolite catalysts for converting vegetable oil to hydrocarbon biofuel [11,18,19]. Karnjanakom et al. [20] found that when Zn was loaded on Al_2O_3, the acidity of the catalyst was promoted. A high acidity plays an important role in the conversion of oxygenates to hydrocarbons. Also, the zinc species might promote the hydrogen transfer during the catalytic upgrading of bio-oil process. The Zn/Al_2O_3 catalyst exhibited a high catalytic activity and long-term stability for the conversion of oxygenates to hydrocarbons, which was related to its acidity and coke resistance properties. There have been a few studies related to the biofuel production over a variety of Al_2O_3 support catalysts, but the report about using Mo and Zn co-modified Al_2O_3 as a catalyst for the hydroprocessing of inedible vegetable oil is lacking.

The objective of this work is to study the hydroprocessing of inedible carinata oil to produce hydrocarbon biofuel in a batch reactor at a temperature of 350 °C. The effect of Mo-Zn/Al_2O_3 catalyst on the product yield and hydrocarbon biofuel properties such as total acid number (TAN) and moisture content was explored and discussed. The catalysts were characterized using a variety of techniques and the composition of the gas produced was analyzed. The possible main reactions for hydroprocessing of carinata oil to hydrocarbons over Mo-Zn/Al_2O_3 catalyst were proposed. In addition, the pressure of the batch reactor was recorded to investigate its initial, maximum and final pressure.

2. Experimental

2.1. Feedstock and catalyst preparation

Carinata (Brassica) oil was provided by Dr. Dwayne Beck from the Dakota Lakes Research Farm, South Dakota, USA. The carinata oil was directly used for hydroprocessing trials without any pretreatment. Aluminum oxide (powder, ≤ 10 μm average particle size, 99.5% trace metals basis) and ammonium molybdate tetrahydrate (99.98% trace metals basis) were purchased from Sigma-Aldrich Inc., Milwaukee, Wisconsin. Zinc chloride was purchased from Fisher Scientific. A series of Mo-Zn/Al_2O_3 catalysts with different Zn/Mo molar ratios (0, 1, 2, 3, ∞) were prepared using a wet impregnation method. For example, Mo-Zn(2)/Al_2O_3 was defined as the Mo-Zn/Al_2O_3 catalyst with the Zn/Mo molar ratio of 2. The aluminum oxide support was impregnated with an aqueous solution of a certain amount of ammonium molybdate tetrahydrate and zinc chloride. The Al_2O_3 support was doped with 4 wt.% Mo to form Mo-Zn(0)/Al_2O_3 (Mo/Al_2O_3) catalyst. Based on Mo/Al_2O_3, the catalysts of Mo-Zn(1)/Al_2O_3, Mo-Zn(2)/Al_2O_3 and Mo-Zn(3)/Al_2O_3 were synthesized through doping a suitable amount of Zn. For catalysts of Mo/Al_2O_3, Mo-Zn(1)/Al_2O_3, Mo-Zn(2)/Al_2O_3 and Mo-Zn(3)/Al_2O_3, the molar ratios of Mo to Al_2O_3 was the same, 0.05. The Al_2O_3 support was doped with 4 wt.% Zn to form Mo-Zn(∞)/Al_2O_3 (Zn/Al_2O_3) catalyst, whose molar ratio of Zn to Al_2O_3 was 0.07. The catalysts were dried at 106 °C for 4 h and then calcined at 550 °C for 4 h. The catalysts were ground into powders using a pestle for hydroprocessing use [18,21].

2.2. Catalyst characterization

The catalysts were characterized using X-ray Diffractometer (XRD), Fourier transform infrared spectroscopy (FT-IR), automated gas adsorption analyzer, and transmission electron microscope (TEM). The phase identification and crystalline structure of Mo-Zn/Al_2O_3 catalysts were determined using an automated multipurpose XRD (SmartLab, Rigaku Corporation) with Cu Kα radiation. The X-ray pattern was scanned from 10° to 90° (2θ) with a step of 0.02° and a scan speed of 2.00°/min, in a continuous mode and an absolute range. The tube voltage and tube current of the X-ray generator were 40 kV and 44 mA, respectively [11,22]. The detail on the procedure of FT-IR, automated gas adsorption analyzer and TEM could be found in our previous research [11,23].

2.3. Hydroprocessing

The hydroprocessing of carinata oil was carried out in a batch reactor (Parr, model 4843) with a heating rate of 5/min. The maximum pressure tolerance of the stainless steel autoclave is 3.44×10^7 Pa (5000 pounds per square inch (psi)). The stirring speed of the turbine paddle stirrer was set as about 1600 rpm. Hydrogen was used to remove the air throughout the reactor system for 5 min, and then it was filled to charge the reactor system until the pressure was 2.07×10^6 Pa (300 psi) at room temperature (25 °C). After that, the hydrogen cylinder was turned off and the autoclave was heated to 350 °C, which was then maintained for 5 h. In each test, 100 g of carinata oil was poured into the autoclave and then 10 g of catalyst was added (there was no catalyst added into the autoclave for no catalyst test). The catalyst-to-oil ratio was selected as 1:10 mainly due to the considerations that the catalyst could be deactivated during the oil hydroprocessing and a large amount of catalyst could increase the cost. Also, it was determined based on our previous research and literature review [24,25]. During each test, the maximum pressure of the reactor system was recorded. After the test, the autoclave was left overnight to cool down to room temperature; then, the final pressure of the reactor system was recorded. A Virgin PTFE (polytetrafluoroethylene) gasket was used to seal the autoclave. The cap screws and connections were tightened properly. The gas leaks in the autoclave after an overnight were very few or negligible. The gas remaining in the reactor system was collected using a gas sampling bag to determine its composition. The mixture of liquid and solid was filtered using a separation funnel to separate the liquid from the solid. The liquid was considered as hydrocarbon biofuel in this study; and the

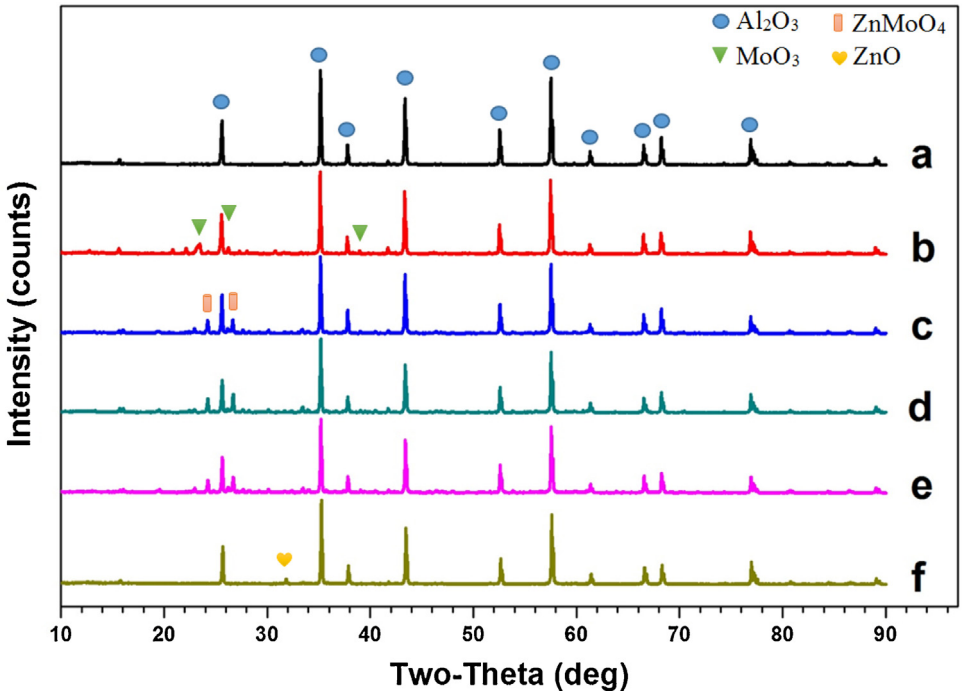

Fig. 1. XRD spectra of catalysts: (a) Al_2O_3; (b) Mo/Al_2O_3; (c) $Mo\text{-}Zn(1)/Al_2O_3$; (d) $Mo\text{-}Zn(2)/Al_2O_3$; (e) $Mo\text{-}Zn(3)/Al_2O_3$; and (f) Zn/Al_2O_3.

solid was considered as used catalyst containing catalyst and coke [4,24]. The used catalyst was washed with excess hexane and then dried at 60 °C overnight. The yields of products were defined by the following formulas (Eqs. (1)-(4)):

$$\text{Yield of coke} = \frac{\text{mass of coke}}{\text{mass of oil feed}} \times 100\% \quad (1)$$

$$\text{Mass of coke} = \text{mass of used catalyst after being washed and dried} - \text{mass of fresh catalyst} \quad (2)$$

$$\text{Yield of gas} = \frac{\text{mass of oil feed} - \text{mass of hydrocarbon biofuel} - \text{mass of coke}}{\text{mass of oil feed}} \times 100\% \quad (3)$$

$$\text{Yield of hydrocarbon biofuel} = \frac{\text{mass of hydrocarbon biofuel}}{\text{mass of oil feed}} \times 100\% \quad (4)$$

2.4. Physicochemical properties

The main physicochemical properties of carinata oil were measured. The obtained hydrocarbon biofuel was characterized by testing its major components, density, moisture content, total acid number, and higher heating value (HHV); and the obtained gas was characterized by testing its composition. The major components of the hydrocarbon biofuel were analyzed using a Gas Chromatography-Mass Spectrometry (GC–MS, Agilent GC-7890A and MSD-5975C) with a hydrogen flow rate of 1.0 mL/min. The capillary column was a 30 m × 0.25 mm × 0.25 μm DB-5MS. 1.0 μL of hydrocarbon biofuel was introduced to the GC–MS through an injection port operated in a splitless mode at 300 °C. The gas chromatograph was programmed at 60 °C for holding 1.0 min, followed by ramp 1 at 5 °C/min to 180 °C for holding 1.0 min, ramp 2 at 10 °C/min to 220 °C for holding 1.0 min, and ramp 3 at 15 °C/min to 280 °C for holding 4.0 min. The major components of hydrocarbon biofuel were identified through a National Institute of Standards and Technology (NIST) mass spectra library and literature [3,23,26–28]. The relative content of the components was determined based on the GC–MS peak area. Density was determined by the ratio of mass to volume of the hydrocarbon biofuel at room temperature. Moisture content was measured using a Karl Fischer Titrator V20 (Mettler Toledo Company), based on ASTM E1064. Total acid number was determined using an Aquamax MicroTan Titrator (G.R. Scientific) in accordance with ASTM D664. HHV was measured using a Calorimeter System (C 2000, IKA-Works, Inc.) according to ASTM D4809. The element analysis of the carinata oil was performed using a CE-440 Elemental Analyzer (Exeter Analytical, Inc.) according to ASTM D4057. The composition of gas was determined using an Agilent GC (7890A) with a 19095P-S25 column of 50 m × 0.53 mm × 15 μm DB-5MS. A flame ionization detector (FID) and a thermal conductivity detector (TCD) were used for the analysis of light hydrocarbons (C_1—C_5), H_2, CO and CO_2. Standard gas mixtures were used for calibration and GC was programmed at 60 °C for holding 3.0 min, followed by ramp 1 at 5 °C/min to 100 °C, and ramp 2 at 10 °C/min to 180 °C for holding 3.0 min [11,18,29].

3. Results and discussion

3.1. Catalyst characterization

3.1.1. XRD analysis

Fig. 1 shows the XRD spectra of Al_2O_3 based catalysts. The diffraction peak characteristics of the Al_2O_3 structure at $2\theta = 25.58°$, 35.15°, 37.78°, 43.36°, 52.55°, 57.50°, 61.30°, 66.52°, 68.21° and 77.23° were observed on the XRD patterns of all six Al_2O_3 based catalysts according to Joint Committee on Power Diffraction Standards (JCPDS) file No. 00-046-1212. These peak positions are in accord with the previously reported Al_2O_3 structure studied by Ayodele et al. [30]. It suggests that the crystalline structure of the

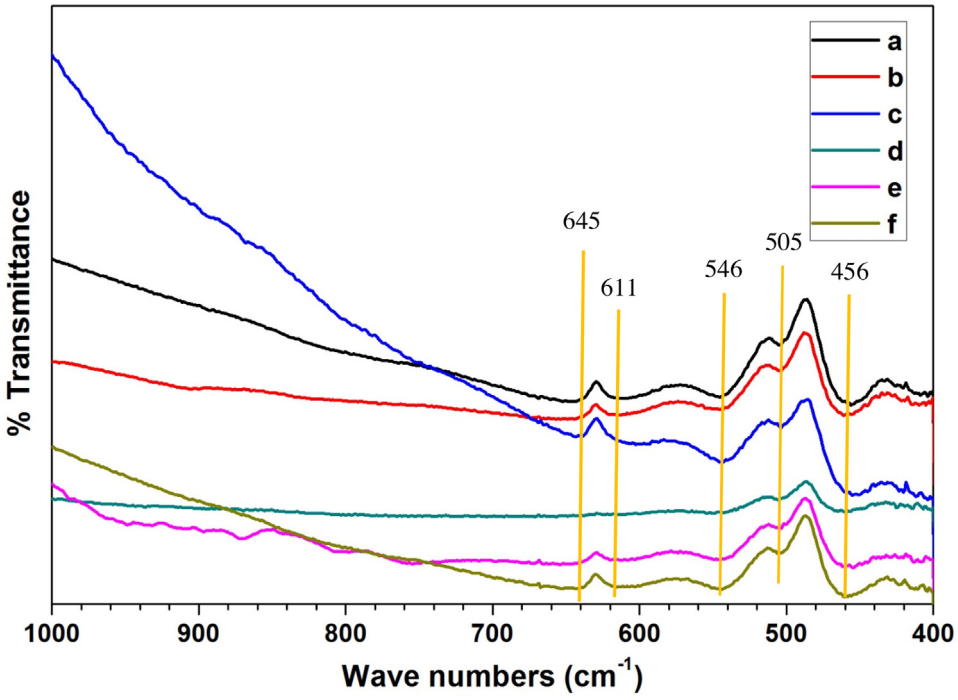

Fig. 2. FTIR of catalysts: (a) Al_2O_3; (b) Mo/Al_2O_3; (c) $Mo\text{-}Zn(1)/Al_2O_3$; (d) $Mo\text{-}Zn(2)/Al_2O_3$; (e) $Mo\text{-}Zn(3)/Al_2O_3$; and (f) Zn/Al_2O_3.

support Al_2O_3 remained constant after the loading of Mo and/or Zn. Mo/Al_2O_3 showed MoO_3 phase at peaks of 23.45°, 26.27° and 39.02° according to JCPDS file No. 00-035-0609 [31]. $Mo\text{-}Zn(1)/Al_2O_3$, $Mo\text{-}Zn(2)/Al_2O_3$ and $Mo\text{-}Zn(3)/Al_2O_3$ showed $ZnMoO_4$ phase at peaks of 24.19° and 26.64° according to JCPDS file No. 01-070-5387. In addition, these three catalysts showed MoO_3 phase at the peak of 39.02°. However, the peak intensities of Al_2O_3 for $Mo\text{-}Zn(1)/Al_2O_3$ were higher than those for $Mo\text{-}Zn(2)/Al_2O_3$ and $Mo\text{-}Zn(3)/Al_2O_3$, which might result from the increase of Zn/Mo molar ratio. Zn/Al_2O_3 showed ZnO phase at the peak of 31.85° according to JCPDS file No. 36–1451 [11].

3.1.2. FT-IR analysis

Fig. 2 shows the FT-IR spectra of Al_2O_3 based catalysts between 1000 cm^{-1} and 400 cm^{-1}. The large broadening bond between 1000 cm^{-1} and 400 cm^{-1} of these catalysts was a characteristic absorption band of alumina. This bond was attributed to stretching vibration of the Al-O bond [32]. The results indicate that the loading of Mo and/or Zn had no significant influence on the framework of the support Al_2O_3, which is consistent with the above XRD result. The FT-IR spectra of Al_2O_3 exhibited two characteristic peaks at around 505 cm^{-1} and 611 cm^{-1} due to the stretching vibrations of Al-O bond [33]. It is obvious that the intensity of characteristic peaks (around 456 cm^{-1}, 505 cm^{-1}, 546 cm^{-1}, 611 cm^{-1} and 645 cm^{-1}) of $Mo\text{-}Zn(2)/Al_2O_3$ was lower than that of other catalysts. One possible explanation could be that metal oxides such as $ZnMoO_4$ and MoO_3 interacted with the surface sites on alumina (e.g. Al^{3+}) to weaken the Al-O bond when the Zn/Mo molar ratio was 2 [34].

3.1.3. N_2 adsorption-desorption analysis

Table 1 lists the adsorption-desorption analysis of Al_2O_3 based catalysts. After the loading of Mo and/or Zn to Al_2O_3, the BET surface area decreased (except $Mo\text{-}Zn(1)/Al_2O_3$). Some of the micropores and mesopores of the support Al_2O_3 were filled up with metal oxides after the metal-loading, which might result in the decrease of the BET surface area [11]. However, some of the mesopores of $Mo\text{-}Zn(1)/Al_2O_3$ were originated from the interparticle voids, which might be due to the aggregation of partial metal oxides deposited on the surface of Al_2O_3 [35]. The average pore diameter of all metal-loading Al_2O_3 catalysts was lower than that of Al_2O_3. One possible explanation could be that some of the micropores and mesopores of the support Al_2O_3 were filled up with metal oxides after the metal-loading. This assumption is in accordance with the result that the total pore volume of metal-loading Al_2O_3 catalysts (except $Mo\text{-}Zn(1)/Al_2O_3$) decreased compared to Al_2O_3. For $Mo\text{-}Zn(1)/Al_2O_3$, some of its mesopores originated from the interparticle voids might cause its equal total pore volume to that of Al_2O_3.

Table 1
Textural properties of the catalysts.

Catalyst	S_{BET}[a] (m^2/g)	$d_{average}$[b] (nm)	Total pore volume (cm^3/g)
Al_2O_3	341.08	3.333	0.28
Mo/Al_2O_3	289.20	3.327	0.24
$Mo\text{-}Zn(1)/Al_2O_3$	358.07	3.17	0.28
$Mo\text{-}Zn(2)/Al_2O_3$	214.47	3.27	0.18
$Mo\text{-}Zn(3)/Al_2O_3$	217.82	3.29	0.18
Zn/Al_2O_3	244.75	3.05	0.19

[a] BET surface area.
[b] Adsorption average pore diameter.

3.1.4. TEM analysis

Fig. 3 shows the TEM images of Al_2O_3 based catalysts. The Al_2O_3 did not show any dark spot since there was no Mo or Zn loading on it. The Mo/Al_2O_3 showed dark spots, which were attributed to the MoO_3 aggregation. The $Mo\text{-}Zn(1)/Al_2O_3$, $Mo\text{-}Zn(2)/Al_2O_3$ and $Mo\text{-}Zn(3)/Al_2O_3$ showed dark spots, which might be attributed to the aggregation of $ZnMoO_4$ and/or MoO_3. The Zn/Al_2O_3 showed dark spots, which were attributed to the ZnO aggregation. Similar TEM result was found by Yuan et al. that $Cu\text{-}Zn/Al_2O_3$ showed dark particles, which were attributed to copper oxide and/or zinc oxide [36]. The TEM results of Al_2O_3 based catalysts are consistent with the above XRD analysis results about the presence of peak phase such as MoO_3, $ZnMoO_4$ and ZnO.

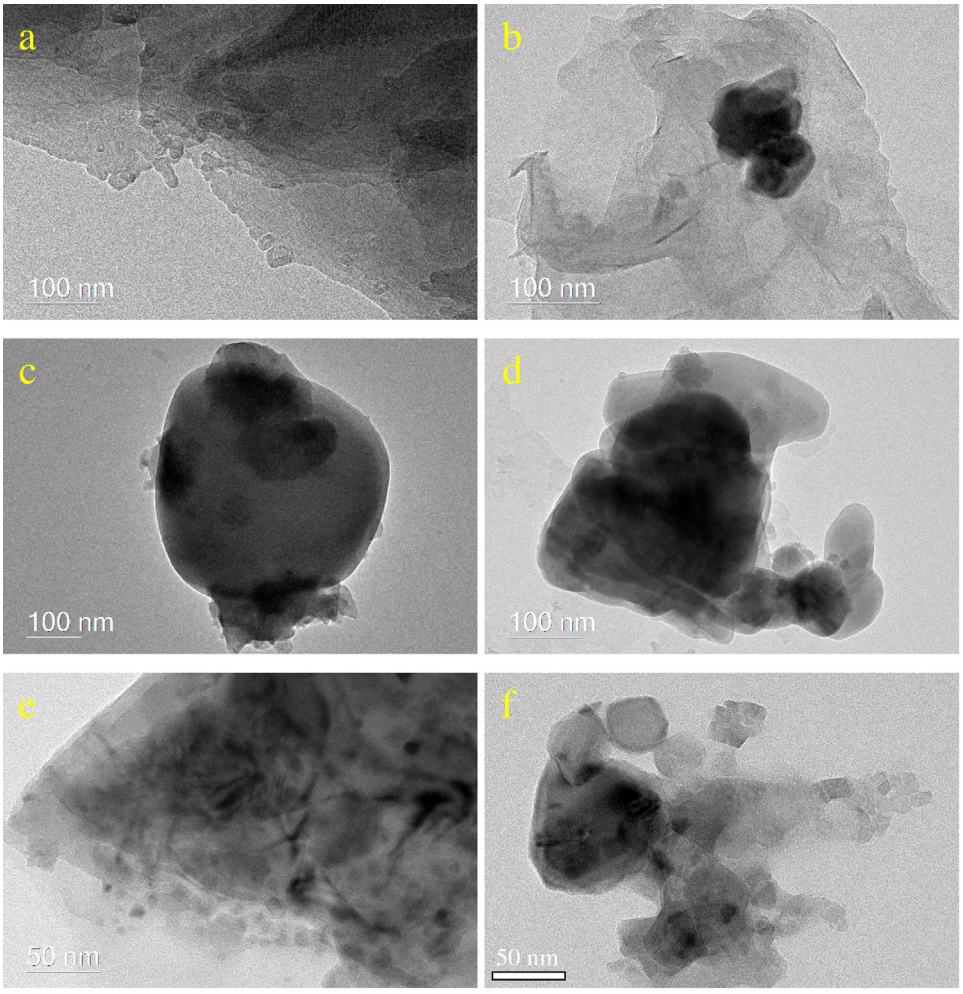

Fig. 3. TEM images of catalysts: (a) Al_2O_3; (b) Mo/Al_2O_3; (c) $Mo\text{-}Zn(1)/Al_2O_3$; (d) $Mo\text{-}Zn(2)/Al_2O_3$; (e) $Mo\text{-}Zn(3)/Al_2O_3$; and (f) Zn/Al_2O_3.

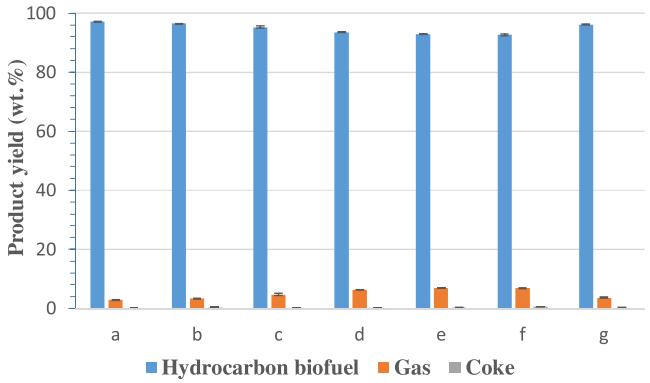

Fig. 4. The product yield obtained over (a) no catalyst; (b) Al_2O_3; (c) Mo/Al_2O_3; (d) $Mo\text{-}Zn(1)/Al_2O_3$; (e) $Mo\text{-}Zn(2)/Al_2O_3$; (f) $Mo\text{-}Zn(3)/Al_2O_3$; and (g) Zn/Al_2O_3.

3.2. The effect of catalyst on product yield

Fig. 4 shows the yield of hydrocarbon biofuel as well as the gas and coke produced at different conditions. Compared to the product obtained over Al_2O_3 based catalysts, the hydrocarbon biofuel yield obtained over no catalyst was higher and the gas yield was lower. The active sites on the Al_2O_3 based catalyst promoted the cracking of carinata oil triglyceride molecules through its pores and external surface to light molecules such as CO_2, which might increase the gas yield, thus decreasing the hydrocarbon biofuel yield. Similar observation was found by Pinto et al. that the presence of HZSM-5 led to an increase in gas yield and a decrease in liquid yield, compared to the absence of catalyst [37]. Multiple reactions including deoxygenation, cracking, decarboxylation and decarbonylation took place during the hydroprocessing of vegetable oil [17]. Compared to the product obtained over Mo and/or Zn loaded Al_2O_3 catalysts, the hydrocarbon biofuel yield obtained over the Al_2O_3 catalyst was higher and the gas yield was lower. This indicates that the introduction of metal ions such as Mo and Zn to Al_2O_3 was helpful to the hydroprocessing of carinata oil, which was due to the availability of the metal (e.g. Mo or Zn) active sites for the hydroprocessing [30].

The hydrocarbon biofuel yield obtained over the Mo-Zn co-loaded Al_2O_3 catalysts was ranging from 92.61% to 93.54%; and the gas yield obtained over these catalysts was ranging from 6.31% to 6.91%. These yields suggest that varying the Zn/Mo molar co-loading ratios (1, 2, 3) on Al_2O_3 has no significant influence on the hydrocarbon biofuel yield and gas yield during the hydroprocessing of carinata oil. The high hydrocarbon biofuel yield was obtained due to the following possible reasons. First, a low reaction temperature (350 °C) might reduce the cracking reaction. Fan et al. [38] found that the composition of the product oil obtained from hydrocracking of Jatropha oil was strongly affected by the reaction temperature. A high reaction temperature favored the cracking reaction rather than the isomerization reaction. Second, the introduction of H_2 was helpful to convert some of the unsaturated triglycerides to saturated triglycerides through hydro-

Table 2
Physicochemical properties of carinata oil.

Physicochemical properties	Carinata oil
Fatty acid composition (relative content, %)	13-Docosenoic acid ($C_{22}H_{42}O_2$): 48.02 Heptadecanoic acid, 16-methyl- ($C_{18}H_{36}O_2$): 19.85 9-Octadecenoic acid, (E)- ($C_{18}H_{34}O_2$): 11.29 9,12,15-Octadecatrienoic acid, (Z,Z,Z)- ($C_{18}H_{30}O_2$): 10.51 Pentadecanoic acid, 14-methyl- ($C_{16}H_{32}O_2$): 7.74 Octacosanoic acid ($C_{28}H_{56}O_2$): 2.60
Element analysis (wt.%)	Carbon: 78.86 ± 0.59 Hydrogen: 11.80 ± 0.10 Nitrogen: 0.24 ± 0.04 *Rest: 9.11 ± 0.66
Density (g/mL)	0.90 ± 0
Moisture content (wt.%)	0.05 ± 0
Total acid number (mg KOH/g)	4.50 ± 0.18
HHV (MJ/kg)	40.28 ± 0.34

* Rest: it contained oxygen and traces of other elements such as Na, S and K.

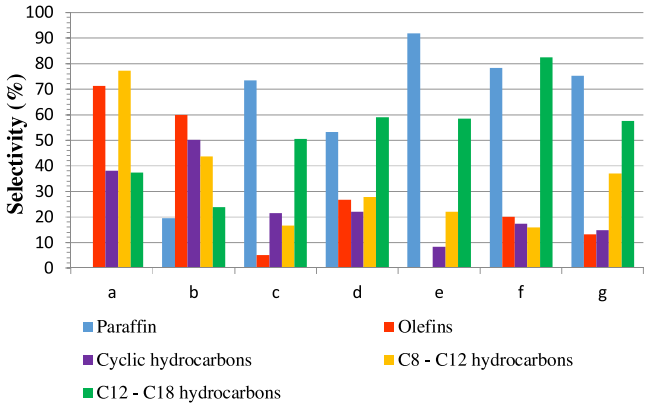

Fig. 5. The selectivity of hydrocarbon biofuel produced over (a) no catalyst; (b) Al_2O_3; (c) Mo/Al_2O_3; (d) Mo-Zn(1)/Al_2O_3; (e) Mo-Zn(2)/Al_2O_3; (f) Mo-Zn(3)/Al_2O_3; and (g) Zn/Al_2O_3. (Selectivity to Paraffin means the fraction of paraffin per total hydrocarbons).

genation reaction. The long chain compounds were then obtained through hydrodeoxygenation reaction. Third, some of the small molecules generated during the carinata oil hydroprocessing might synthesize to produce large molecules that became liquid. The hydrocarbon biofuel yield obtained over Mo-Zn co-loaded Al_2O_3 was higher than the total organic product yield (83.4% – 93.3%) obtained by the hydrotreating of sunflower oil over CoMo/Al_2O_3 catalyst at the pressure of 40–60 bar, studied by Krar et al. [17]. In addition, the gas yield obtained over Mo-Zn co-loaded Al_2O_3 was in the range of the gaseous product yield (4.2% – 10.5%) obtained by the hydrotreating of sunflower oil over CoMo/Al_2O_3 catalyst, studied by Krar et al. [17]. The coke yield obtained over no catalyst was zero and the coke yield obtained over Al_2O_3 based catalysts was lower than 0.60%, which could be considered negligible. Zarchin et al. [12] found that negligible coke was generated during the hydroprocessing of soybean oil over nickel-phosphide supported catalysts. The used Al_2O_3 based catalysts might be collected and calcined to remove coke for further catalytic use.

3.3. The effect of catalyst on physicochemical properties of products

3.3.1. Physicochemical properties of hydrocarbon biofuel

The main physicochemical properties of carinata oil are shown in Table 2. Carinata oil mainly contained unsaturated fatty acids including 13-docosenoic acid ($C_{22}H_{42}O_2$), 9-octadecenoic acid, (E)- ($C_{18}H_{34}O_2$), and 9,12,15-octadecatrienoic acid, (Z,Z,Z)- ($C_{18}H_{30}O_2$). These fatty acids varied in the extent of unsaturation and in the carbon chain length. Table 3 shows the main components of hydrocarbon biofuel produced at different conditions. Due to the large number of molecules in the hydrocarbon biofuel, the components were grouped into acids, alcohols, aldehydes, esters, hydrocarbons, ketones and other. The hydrocarbon biofuels usually contained hydrocarbons and oxygen-containing compounds such as acids, alcohols and esters. Pinto et al. [37] also found the similar liquid composition including hydrocarbons, fatty acids and glycerides after the hydrotreating of pomace oil. The hydrocarbon biofuel produced over Mo/Al_2O_3 contained a high amount of ketone compounds, which might be due to the redox properties of MoO_3 catalyzing the oxidation of olefins to ketones. It was proposed that an oxygen atom located on the surface of MoO_3 reacted with olefins to produce an oxygenated product [39]. The acid content of hydrocarbon biofuel produced over no catalyst was higher than that obtained over Al_2O_3 based catalysts. The use of Al_2O_3 based catalysts promoted the fatty acid destruction. The destruction of oxygen-containing compounds through deoxygenation reactions was observed [37]. The hydrocarbon biofuel produced over Mo and/or Zn loaded Al_2O_3 catalysts contained a lower acid content than that over Al_2O_3 catalyst. A suitable metal (e.g. Mo, Zn, Fe and Cu) loading amount on Al_2O_3 could promote the acidity of the catalyst. The acid sites of the catalyst could promote the deoxygenation reaction to produce hydrocarbons [14,20].

The hydrocarbon content of hydrocarbon biofuel produced over no catalyst was lower than that obtained over Al_2O_3 based catalysts. One possible explanation could be that the Al_2O_3 based catalysts promoted the decarboxylation reaction [37]. The hydrocarbon biofuel produced over Mo-Zn(2)/Al_2O_3 contained the highest hydrocarbon content (81.05%) and the lowest ester content. Romero et al. [40] studied that the highest hydrocarbon content (81.08%) of biofuel was obtained from the deoxygenation of non-edible Jatropha Curcas oil over the hydrotalcite catalyst. The hydrocarbon content of the hydrocarbon biofuel produced over Mo and Zn loaded Al_2O_3 catalysts tended to increase with the increase of the Zn/Mo molar ratio, but then decreased when the Zn/Mo molar ratio was 3. One possible reason is that a higher Zn/Mo molar ratio might cause an aggregation of ZnO particles, which might accelerate the deactivation of the catalyst [11]. Although carinata oil was composed mainly by fatty acids of 13-docosenoic acid ($C_{22}H_{42}O_2$) and heptadecanoic acid, 16-methyl- ($C_{18}H_{36}O_2$), the hydrocarbon biofuel produced was not composed mainly by C21 and/or C17 hydrocarbons. One possible reason is that cracking was a significant reaction taking place during the hydroprocessing of carinata oil. Some of the hydrocarbon biofuels contained isomers such as $C_{14}H_{30}$ and $C_{15}H_{32}$. Fig. 5 shows the selectivity of hydrocarbon biofuel produced at different conditions. The hydrocarbon biofuel produced over Mo-Zn(2)/Al_2O_3 showed the highest selectivity to paraffin, but the lowest selectivity to olefins and the lowest selectivity to cyclic. The hydrocarbon biofuel produced over no catalyst showed the highest selectivity to olefins and the hydrocarbon biofuel produced over Al_2O_3 showed the highest selectivity to cyclic. Different Al_2O_3 based catalysts had a certain influence on the hydrocarbon distribution of hydrocarbon biofuel. The hydrocarbon biofuel produced over Mo-Zn(2)/Al_2O_3 contained the hydrocarbons between C_6 and C_{36}, where hexadecane ($C_{16}H_{34}$) accounted the most. Also, the hydrocarbon biofuel produced over Mo-Zn(2)/Al_2O_3 contained a high amount of C6–C11 hydrocarbons, which might be because the loading of Mo and Zn to Al_2O_3 promoted some of the cracking reactions. Srifa et al. [16] found the C8–C14 hydrocarbons obtained during the hydrodeoxygenation of palm oil over Ni/Al_2O_3 and Co/Al_2O_3 catalysts, which had partial selectivity to C—C cleavage. The hydrocarbon biofuel produced over no catalyst showed a higher selectivity to gas oil

Table 3
Main components of hydrocarbon biofuel produced at different conditions.

Compounds	Relative content (%)						
	No catalyst	Al_2O_3	Mo/Al_2O_3	$Mo\text{-}Zn(1)/Al_2O_3$	$Mo\text{-}Zn(2)/Al_2O_3$	$Mo\text{-}Zn(3)/Al_2O_3$	Zn/Al_2O_3
Acids	11.25	10.84	5.73	4.62	4.54	3.09	5.37
Alcohols	9.09	9.96	7.25	5.78	7.57	7.55	6.72
Aldehydes	5.40	–	–	1.54	–	–	–
Esters	13.79	9.06	12.22	16.72	1.77	8.10	24.27
Hydrocarbons	18.67	37.26	47.12	63.39	81.05	73.19	46.62
Ketones	6.91	1.93	12.96	1.69	–	–	1.43
Other[a]	34.90	30.97	14.73	6.25	5.07	8.07	15.59

[a] Other: the compounds that did not belong to the above groups, not including unidentified compounds.

(C8–C12 hydrocarbons) than that produced over Al_2O_3 based catalysts. However, the hydrocarbon biofuel produced over no catalyst showed a lower selectivity to diesel fuel (C12–C18 hydrocarbons) than that produced over Mo and/or Zn loaded Al_2O_3 catalysts. Hydrodeoxygenation, decarboxylation and decarbonylation were three possible reaction pathways for the oxygen removal from carinata oil triglyceride molecules [17]. The hydrocarbon biofuels produced contained a certain amount of long chain hydrocarbons (> C15), indicating that they need further cracking if they are used as light hydrocarbon fuels (C6–C12) like gasoline.

Table 4 shows the main physicochemical properties of hydrocarbon biofuels produced at different conditions. After the hydroprocessing of carinata oil, its density decreased and HHV increased. During the hydroprocessing, carinata oil triglyceride molecules were decomposed to fatty acids, which were then formed to light fraction composition through chemical reactions such as deoxygenation and decarboxylation [11,37]. The density of the hydrocarbon biofuel produced over no catalyst was higher than that obtained over Al_2O_3 based catalysts, which was due to the catalyst use promoting the fatty acid destruction. The density of the hydrocarbon biofuels produced over Al_2O_3 based catalysts was lower or equal to the density of hydrotreated waste cooking oil (0.87 g/mL) produced over CoMoS catalyst at 340 °C studied by Zhang et al. [41]. The higher heating values of the hydrocarbon biofuels produced over Al_2O_3 based catalysts were in the range of 40–44 MJ/kg, which were the heating values of biofuels obtained from the deoxygenation of Jatropha Curcas oil over the alumina or hydrotalcite catalyst reported by Romero et al. [40].

However, after the hydroprocessing of carinata oil, its moisture content increased and total acid number increased. Water was a byproduct during the hydroprocessing of carinata oil through hydro-decarbonylation and/or hydro-dewatering [12,13]. The hydrocarbon biofuel produced over $Mo\text{-}Zn(2)/Al_2O_3$ contained the lowest moisture content (0.22%), but it was higher than the moisture content of pure hydrotreated vegetable oil (< 0.02%) studied by Engman et al. [42]. This means more research is needed in the future to reduce the moisture content of hydrocarbon biofuel. The total acid number of hydrocarbon biofuels was higher than that of carinata oil, which might be due to the decomposition of carinata oil triglyceride molecules to fatty acids. The higher the total acid number, the higher the formation of acidic products that cause the biofuel tank corrosion [19]. The total acid number of the hydrocarbon biofuel produced over no catalyst was higher than that obtained over Al_2O_3 based catalysts. This result is consistent with the above GC–MS results of hydrocarbon biofuels that the acid content of the hydrocarbon biofuel produced over no catalyst was higher than that obtained over Al_2O_3 based catalysts. The catalyst support plays an important role in the oxygen removal during the hydroprocessing of oil. For example, Al_2O_3 has a catalytic activity in the hydroprocessing reactions due to its Lewis acid sites [41]. Some of the fatty acids formed alcohols, aldehydes and ketones through hydrodeoxygenation. Hydrodeoxygenation took place on the active sites of the Al_2O_3 based catalysts. Similarly, Zhang et al. [41] found that fatty acids were transferred to alcohols/aldehydes through the hydrodeoxygenation reaction taking place on the active sites of CoMoS catalyst. The total acid number of hydrocarbon biofuels obtained over Mo and/or Zn loaded Al_2O_3 catalysts was in the range of 86.80–134.55 mg KOH/g, which was lower than that of hydrocarbon fuel (about 140 mg KOH/g) produced from hydrocracking of soybean oil over NiMo nitride catalyst after six days, studied by Wang et al. [43]. The high total acid number of hydrocarbon biofuel was caused by its large amounts of carboxyl acids [43]. Co-loading Mo and Zn to Al_2O_3 was helpful to reduce the moisture content, density and total acid number and to increase the HHV of the hydrocarbon biofuel.

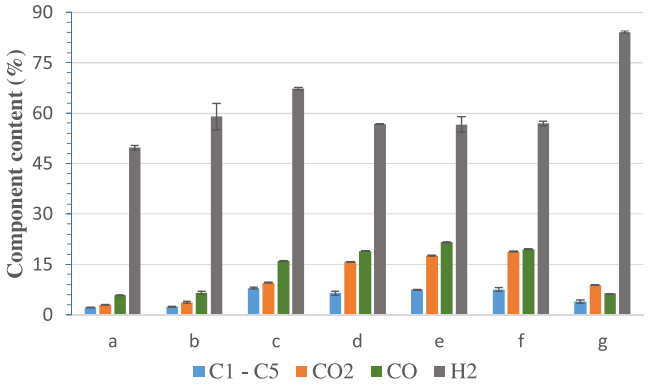

Fig. 6. The component content of gas produced over (a) no catalyst; (b) Al_2O_3; (c) Mo/Al_2O_3; (d) $Mo\text{-}Zn(1)/Al_2O_3$; (e) $Mo\text{-}Zn(2)/Al_2O_3$; (f) $Mo\text{-}Zn(3)/Al_2O_3$; and (g) Zn/Al_2O_3.

3.3.2. Component analysis of gas

The distribution of components of gas produced from the hydroprocessing of carinata oil is shown in Fig. 6. The gas produced contained light hydrocarbons (CH_4, C_2H_6, C_2H_4, C_3H_8, C_3H_6, C_4H_{10}, C_4H_8, C_5H_{12}), CO_2, CO and H_2. Hydro-decarbonylation removed the carboxyl groups from carinata oil fatty acids by forming CO, hydrocarbons and water, while hydro-decarboxylation produced CO_2 and hydrocarbons through the removal of carboxyl groups [12,13,19,44]. Some of the hydrocarbons produced were cracked to light hydrocarbons such as CH_4 and C_2H_6 through cracking reactions [41,45,46]. Compared to the component distribution of gas obtained over Al_2O_3 based catalysts, the CO_2 content and the CO content produced over no catalyst were lower. This indicates that the decarboxylation and decarbonylation reactions were promoted in the presence of Al_2O_3 based catalysts. Decarbonylation was favored than decarboxylation during the hydroprocessing of carinata oil, except over Zn/Al_2O_3 catalyst. Decarbonylation was favored over $Mo\text{-}Zn(2)/Al_2O_3$ catalyst and decarboxylation was favored over $Mo\text{-}Zn(3)/Al_2O_3$ catalyst. Pinto et al. [37] also observed that the decarboxylation reaction was promoted in the presence of

Table 4
Physicochemical properties of hydrocarbon biofuel produced at different conditions.

Treatment	Moisture content (wt.%)	Density (g/mL)	Total acid number (mg KOH/g)	HHV (MJ/kg)
No catalyst	0.44 ± 0.01	0.88 ± 0.01	161.00 ± 2.83	41.02 ± 0.01
Al_2O_3	0.46 ± 0.01	0.86 ± 0.03	160.65 ± 1.34	40.79 ± 0.16
Mo/Al_2O_3	0.41 ± 0.02	0.87 ± 0.01	134.55 ± 4.03	42.06 ± 0.07
$Mo\text{-}Zn(1)/Al_2O_3$	0.26 ± 0.01	0.84 ± 0.02	101.40 ± 2.40	42.79 ± 0.08
$Mo\text{-}Zn(2)/Al_2O_3$	0.22 ± 0.01	0.85 ± 0.01	92.65 ± 4.17	43.25 ± 0.05
$Mo\text{-}Zn(3)/Al_2O_3$	0.39 ± 0.01	0.85 ± 0.01	86.80 ± 0.57	43.41 ± 0.03
Zn/Al_2O_3	1.44 ± 0.04	0.86 ± 0.01	134.10 ± 3.96	41.35 ± 0.07

Table 5
The reactor pressure during the hydroprocessing of carinata oil.

Treatment	Initial pressure (psi)	Maximum pressure (psi)	Final pressure (psi)
No catalyst	300	705 ± 7.07	330 ± 0
Al_2O_3	300	685 ± 7.07	305 ± 21.21
Mo/Al_2O_3	300	710 ± 14.14	275 ± 7.07
$Mo\text{-}Zn(1)/Al_2O_3$	300	730 ± 14.14	250 ± 14.14
$Mo\text{-}Zn(2)/Al_2O_3$	300	815 ± 7.07	265 ± 7.07
$Mo\text{-}Zn(3)/Al_2O_3$	300	840 ± 0	260 ± 0
Zn/Al_2O_3	300	790 ± 0	280 ± 0

$CoMo/Al_2O_3$ catalyst. Compared to the component distribution of gas obtained over Mo and/or Zn loaded Al_2O_3 catalysts, the CO_2 content produced over Al_2O_3 were lower. The sum content of CO_2 and CO was the highest when $Mo\text{-}Zn(2)/Al_2O_3$ was used as the catalyst. The production of CO_2 and CO was helpful to remove the oxygen atoms from the carinata oil triglyceride molecules. Compared to the component distribution of gas obtained over Al_2O_3 based catalysts, the sum content of light hydrocarbons (C_1–C_5) produced over no catalyst was lower. Compared to the component distribution of gas obtained over Mo and/or Zn loaded Al_2O_3 catalysts, the sum content of light hydrocarbons produced over Al_2O_3 was lower. One possible reason is that the loading of Mo and/or Zn to Al_2O_3 promoted some of the cracking reactions. Srifa et al. [16] found that the formation of some light hydrocarbons such as C_2H_6 and C_3H_8 could be associated with the cracking reactions during the deoxygenation of palm oil over monometallic catalysts.

3.4. The effect of catalyst on the reactor pressure

Table 5 shows the batch reactor pressure during the hydroprocessing of carinata oil at different conditions. Compared to the final pressure obtained over Al_2O_3 based catalysts, the final pressure obtained over no catalyst was higher. It indicates that the use of Al_2O_3 based catalysts led to higher hydrogen consumption. The Al_2O_3 is usually used as a catalyst for the hydroprocessing of vegetable oil and bio-oil due to its high acidity [20].The promotion of the hydro-decarbonylation and hydro-decarboxylation over Al_2O_3 based catalysts might cause the more hydrogen consumption and lead to the higher amounts of light molecules such as hydrocarbons. Similar observation was found by Pinto et al. [37] that the use of catalysts such as $CoMo/Al_2O_3$ and HZSM-5 resulted in higher hydrogen consumption during the hydrotreating of pomace oil in a batch reactor. The introduction of Mo and/or Zn on Al_2O_3 resulted in a decrease of the final pressure of the batch reactor to 250–280 psi. A certain amount of Mo and/or Zn loading on Al_2O_3 might increase the catalyst acidity, which could promote the hydrodeoxygenation reaction [14,20]. Also, the Zn^{2+} might make the hydrodeoxygenation reaction of the C=O groups more efficiently [24]. Under this situation, more hydrogen could be consumed to produce more hydrocarbons. This indicates that $Mo\text{-}Zn/Al_2O_3$ catalysts benefited the hydroprocessing of carinata oil for hydrocarbon biofuel production. Co-loading Mo and Zn to Al_2O_3 decreased the final pressure of the reactor. In addition, the maximum pressure obtained over Mo-Zn co-loaded Al_2O_3 was higher than that obtained at other conditions.

4. Conclusions

Non-food carinata oil can be hydroprocessed to produce hydrocarbon biofuel over $Mo\text{-}Zn/Al_2O_3$ catalyst in a batch reactor. The crystalline structure of the Al_2O_3 catalyst is not changed significantly after the introduction of Mo and/or Zn. The hydrocarbon biofuels produced over $Mo\text{-}Zn/Al_2O_3$ catalysts mainly contain hydrocarbons, but also contain a certain amount of oxygen containing compounds such as acids, alcohols and esters. The co-loading of Mo and Zn on Al_2O_3 is helpful to improve the catalytic performance and some of the properties (e.g. moisture content, density, total acid number and higher heating value) of hydrocarbon biofuel. The highest hydrocarbon content of 81.05% is obtained when the Zn/Mo molar ratio is 2:1. Compared to hydroprocessing with no catalyst, the use of Al_2O_3 based catalysts promotes the hydro-decarbonylation and hydro-decarboxylation. Subsequently, the use of Al_2O_3 based catalysts increases the gas yield, thus decreasing the hydrocarbon biofuel yield. Due to the high hydrocarbon biofuel yield (> 92%), the coke yield obtained from the hydroprocessing of carinata oil could be considered negligible.

In the future, the hydroprocessing of non-food vegetable oil could be optimized based on the reaction temperature, catalyst species, hydrogen pressure and catalyst-to-oil ratio. The hydrocarbon biofuel produced could be treated further such as by distillation to separate hydrocarbons from oxygen-containing compounds. In addition, the used Al_2O_3 based catalysts might be collected and calcined to remove coke for further hydroprocessing use.

Acknowledgements

This study was funded by the U.S. Department of Transportation through NC Sun Grant Initiative under Grant No. SA0700149. The authors would like to thank Dr. Dwayne Beck for providing carinata oil, Dr. Qiquan Qiao and Mr. Ashish Dubey for helping in the XRD and FTIR measurement, and Dr. Phil Ahrenkiel for helping in the TEM measurement. The XRD equipment is supported by the NSF MRI grant (Award No. 1229577). All the support in experiment from Mr. Yong Yu is gratefully acknowledged. However, only the authors are responsible for the opinions expressed in this paper and for any possible error.

References

[1] C. Stamigna, D. Chiaretti, E. Chiaretti, P.P. Prosini, Biomass Bioenerg. 39 (2012) 478–483.
[2] X. Zhao, L. Wei, J. Julson, AIMS Energy 2 (2014) 193–209.
[3] S. Cheng, L. Wei, X. Zhao, E. Kadis, J. Julson, Energy Technol. (2016) http://dx.doi.org/10.1002/ente.201500452.
[4] S. Cheng, L. Wei, X. Zhao, E. Kadis, Y. Cao, J. Julson, Z. Gu, N. Biotechnol. 33 (2016) 440–448.
[5] H.L. Sieverding, X. Zhao, L. Wei, J.J. Stone, J. Environ. Qual. 45 (2016) 967–976.
[6] S. Cheng, L. Wei, X. Zhao, Y. Shen, Y. Yu, L. Jing, ASABE Ann. Int. Meeting (2015) 152167800 http://dx.doi.org/10.13031/aim.20152167800.

[7] D.C. Taylor, K.C. Falk, C.D. Palmer, J. Hammerlindl, V. Babic, E. Mietkiewska, A. Jadhav, E.F. Marillia, T. Francis, T. Hoffman, E.M. Giblin, V. Katavic, W.A. Keller, Biofuels. Bioprod. Biorefin. 4 (2010) 538–561.
[8] A.C. Drenth, D.B. Olsen, P.E. Cabot, J.J. Johnson. Fuel 136 (2014) 143–155.
[9] E.F. Marillia, T. Francis, K.C. Falk, M. Smith, D.C. Taylor, Biocatal. Agr. Biotechnol. 3 (2014) 65–74.
[10] T.V. Rao, M.M. Clavero, M. Makkee, ChemSusChem 3 (2010) 807–810.
[11] X. Zhao, L. Wei, S. Cheng, Y. Huang, Y. Yu, J. Julson, Fuel Process. Technol. 139 (2015) 117–126.
[12] R. Zarchin, M. Rabaev, R. Vidruk-Nehemya, M.V. Landau, M. Herskowitz, Fuel 139 (2015) 684–691.
[13] C. Wang, Z. Tian, L. Wang, R. Xu, Q. Liu, W. Qu, H. Ma, B. Wang, ChemSusChem 5 (2012) 1974–1983.
[14] R. Sun, S. Shen, D. Zhang, Y. Ren, J. Fan, Energy Fuels 29 (2015) 7005–7013.
[15] V.A. Yakovlev, S.A. Khromova, O.V. Sherstyuk, V.O. Dundich, D.Y. Ermakov, V.M. Novopashina, M.Y. Lebedev, O. Bulavchenko, V.N. Parmon, Catal. Today 144 (2009) 362–366.
[16] A. Srifa, K. Faungnawakij, V. Itthibenchapong, S. Assabumrungrat, Chem. Eng. J. 278 (2015) 249–258.
[17] M. Krár, S. Kovács, D. Kalló, J. Hancsók, Bioresour. Technol. 101 (2010) 9287–9293.
[18] X. Zhao, L. Wei, J. Julson, Z. Gu, Y. Cao, Korean J. Chem. Eng. 32 (2015) 1528–1541.
[19] X. Zhao, L. Wei, S. Cheng, Y. Cao, J. Julson, Z. Gu, Appl. Catal. A: Gen. 507 (2015) 44–55.
[20] S. Karnjanakom, G. Guan, B. Asep, X. Du, X. Hao, J. Yang, C. Samart, A. Abudula, RSC Adv. 5 (2015) 83494–83503.
[21] S. Cheng, L. Wei, X. Zhao, Energy Sources Part A (2015) http://dx.doi.org/10.1080/15567036.2015.1065298.
[22] Q. Liu, Y. Zhou, M. Wang, X. Zhao, Y. Lin, J. Alloys Compd. 548 (2013) 161–165.
[23] X. Zhao, L. Wei, J. Julson, Q. Qiao, A. Dubey, G. Anderson, N. Biotechnol. 32 (2015) 300–312.
[24] Y. Huang, L. Wei, X. Zhao, S. Cheng, J. Julson, Y. Cao, Z. Gu, Energ. Convers. Manage. 115 (2016) 8–16.
[25] A. Hart, M. Greaves, J. Wood, Chem. Eng. J. 282 (2015) 213–223.
[26] S. Cheng, L. Wei, X. Zhao, Y. Huang, D. Raynie, C. Qiu, J. Kiratu, Y. Yu, AIMS Energy 3 (2015) 227–240.
[27] X. Zhao, L. Wei, J. Julson, Y. Huang, J. Sustain. Bioenergy Syst. 4 (2014) 199–214.
[28] Y. Huang, L. Wei, J. Julson, Y. Gao, X. Zhao, J. Anal. Appl. Pyrolysis 111 (2015) 148–155.
[29] X. Zhao, L. Wei, S. Cheng, J. Julson, G. Anderson, K. Muthukumarappan, C. Qiu, J. Renew. Sustain. Ener. 8 (2016) 013109.
[30] O.B. Ayodele, O.S. Togunwa, H.F. Abbas, W.M.A.W. Daud, Energ. Convers. Manage. 88 (2014) 1104–1110.
[31] L. Chibane, M.S. Belkaid, M. Pasquinelli, H. Derbal-Habak, J.J. Simon, D. Hocine, J. Mater. Sci. Eng. B 3 (2013) 418–422.
[32] T.M. Costa, M.R. Gallas, E.V. Benvenutti, J.A. da Jornada, J. Phys. Chem. B 103 (1999) 4278–4284.
[33] J.M. Saniger, Mater. Lett. 22 (1995) 109–113.
[34] M.A. Vuurman, D.J. Stufkens, A. Oskam, G. Deo, I.E. Wachs, J. Chem. Soc. Faraday T. 92 (1996) 3259–3265.
[35] S. Wang, Q. Yin, J. Guo, B. Ru, L. Zhu, Fuel 108 (2013) 597–603.
[36] P. Yuan, Z. Liu, W. Zhang, H. Sun, S. Liu, Chinese J. Catal. 31 (2010) 769–775.
[37] F. Pinto, F.T. Varela, M. Gonçalves, R.N. André, P. Costa, B. Mendes, Fuel 116 (2014) 84–93.
[38] K. Fan, J. Liu, X. Yang, L. Rong, Int. J. Hydrogen Energ. 39 (2014) 3690–3697.
[39] T. Prasomsri, T. Nimmanwudipong, Y. Román-Leshkov, Energy Environ. Sci. 6 (2013) 1732–1738.
[40] M.J. Romero, A. Pizzi, G. Toscano, B. Bosio, E. Arato, Chem. Eng. Trans. 37 (2014) 883–888.
[41] H. Zhang, H. Lin, W. Wang, Y. Zheng, P. Hu, Appl. Catal. B: Environ. 150 (2014) 238–248.
[42] M.A. Engman, T. Hartikka, M. Honkanen, U. Kiiski, M. Kuronen, S. Mikkonen, P. Saikkonen, Hydrotreated Vegetable Oil (HVO)-premium Renewable Biofuel for Diesel Engines, Espoo, Finland, 2014, pp. 1–55 (copy available at https://www.neste.com/sites/default/files/attachments/hvo_handbook_original_2014.pdf).
[43] H. Wang, S. Yan, S.O. Salley, K.S. Ng, Ind. Eng. Chem. Res. 51 (2012) 10066–10073.
[44] W. Kiatkittipong, S. Phimsen, K. Kiatkittipong, S. Wongsakulphasatch, N. Laosiripojana, S. Assabumrungrat, Fuel Process. Technol. 116 (2013) 16–26.
[45] X. Zhao, L. Wei, S. Cheng, J. Julson, Ind. Crop. Prod. 77 (2015) 516–526.
[46] A. Srifa, K. Faungnawakij, V. Itthibenchapong, N. Viriya-Empikul, T. Charinpanitkul, S. Assabumrungrat, Bioresour. Technol. 158 (2014) 81–90.